

Removing the influence of a group variable in high-dimensional predictive modelling

Emanuele Aliverti¹, Kristian Lum², James E. Johndrow³, and David B. Dunson⁴

¹Department of Statistical Sciences, University of Padova,
via Cesare Battisti 241, Padova, Italy
email: aliverti@stat.unipd.it

²Human Rights Data Analysis Group, San Francisco

³Department of Statistics, Stanford University

⁴Department of Statistical Science, Duke University

Abstract

Predictive modelling relies on the assumption that observations used for training are representative of the data that will be encountered in future samples. In a variety of applications, this assumption is severely violated, since observational training data are often collected under sampling processes which are systematically biased with respect to group membership. Without explicit adjustment, machine learning algorithms can produce predictions that have poor generalization error with performance that varies widely by group. We propose a method to pre-process the training data, producing an adjusted dataset that is independent of the group variable with minimum information loss. We develop a conceptually simple approach for creating such a set of features in high dimensional settings based on a constrained form of principal components analysis. The resulting dataset can then be used in any predictive algorithm with the guarantee that predictions will be independent of the group variable. We develop a scalable algorithm for implementing the method, along with theory support in the form of independence guarantees and optimality. The method is illustrated on some simulation examples and applied to two real examples: removing machine-specific correlations from brain scan data, and removing race and ethnicity information from a dataset used to predict recidivism.

Keywords: Constrained optimisation; Criminal justice; Neuroscience; Orthogonal predictions; Predictive modelling; Singular value decomposition; ℓ -1 norm.

1 INTRODUCTION

Modern statistical and machine learning applications often rely on large datasets constructed by automated systems; for example, web scraping results from a search term or aggregating publicly accessible information, such as images and online articles. Alternatively, data may be collected within observational studies for a convenience sample of individuals, and interest is on detecting relationships between features and outcome variables; for example, disease or behavior. Such processes create datasets in which the sampling mechanism is complex, unknown, and often subject to some form of systematic bias (Dunson, 2018).

When selection bias exists in the sampling mechanism, inferences or predictions produced using the data often encode spurious associations. There is growing recognition that machine learning algorithms will reproduce and often amplify sampling bias in the data upon which they were trained (e.g. Angwin et al., 2016; Zech et al., 2018; Dunson, 2018). For example, racial bias in police records can be propagated to predictive algorithms trained on these data (Lum and Isaac, 2016). Often in such settings there is concern about sampling bias with respect to a key group membership variable, such as ethnicity, gender or a blocking factor in scientific studies (e.g. the clinical facility in multisite study designs, or the machine on which an assay was performed). Motivated by this problem, we propose a method to adjust high-dimensional datasets in order to remove associations between covariates of interest and group membership, and provide predictions that are free from the effect of sampling bias.

A popular and important application for automated predictions is disease recognition from medical imaging data, such as radiography, ultrasonography and brain scans. Modern machine learning can obtain impressive predictive performance, similar to or better than expert practitioners in the field (e.g. Obermeyer and Emanuel, 2016; Wang and Summers, 2012). Unfortunately, it is virtually impossible to determine and describe the sampling mechanism of such complex data, which contain millions of records collected across different regions, clinical facilities, and equipment. Zech et al. (2018) recently showed that radiographic image data encoded information on the specific hospital system from which the data were collected, likely because different systems tended to use different imaging equipment. When these data

were used to train a model for pneumonia screening, the model learned to associate these hospital-specific characteristics to the outcome of interest. The model’s heavy reliance on such associations jeopardizes the generalizability of the results. This issue is also detrimental for in-sample evaluation, since regarding such associations as risk factors for the outcome of interest is clearly misleading.

Another area in which unwanted associations arise is in criminal justice data. For example, there has been much recent attention on the use of criminal risk assessment models, many of which use demographic, criminal history, and other information to predict whether someone who has been arrested will be re-arrested in the future. These predictions then inform decisions on pre-trial detention, sentencing, and parole. In practice, the data used to train the models are based on arrest records, which are well known to be subject to racial bias (Simoiu et al., 2017; Rudovsky, 2001; Bridges and Crutchfield, 1988; Lum, 2017). When risk assessment models are trained using these data, the end result is that racial minority groups tend to be systematically assigned to higher risk categories on average (Lum and Johndrow, 2016; Angwin et al., 2016).

In this article we focus on developing data pre-processing methods to remove the influence of group membership variables, such as hospital id or racial group. There are several application areas in which datasets are pre-processed in order to remove or obscure specific information. For example, in data confidentiality, there is strong interest in releasing synthetic datasets which minimise the probability to disclose respondents’ identities (Reiter, 2005; Raghunathan et al., 2003). Our work is also closely related to recent methods on data pre-processing in the “algorithmic fairness” literature, where one of the crucial aims is to create datasets which produce predictions that are independent of sensitive variables, such as race or ethnicity or gender (e.g. Feldman et al., 2015; Kamiran and Calders, 2012; Lum and Johndrow, 2016)

The main advantage of our contribution is its simplicity and scalability to a large number of covariates (p), particularly when p is greater than the number of observations n . In this sense, it is particularly well-suited to applications like brain imaging, in which the observed covariates are high-dimensional. It also has significant advantages in the case of highly collinear predictors, which is very common in applications. Moreover, we will show that the solution we propose has theoretical guarantees, both in terms of optimal dimension reduction and statistical parity under a linearity condition.

Our method is motivated by the reliance on very high-dimensional data, such as medical imaging and

“omic” data, for an increasing number of prediction tasks. As previously described, such type of data may encode unnecessary or detrimental correlations that threaten the generalizability of models trained with the data. Removing these associations will be important to ensure that complex prediction models are relying on reliable features that will generalize across a wide variety of patient populations, not just artifacts of the data collection process.

2 GENERATING DATA ORTHOGONAL TO GROUPS

2.1 *Notation and setup*

Let X denote an $n \times p$ data matrix of p features measured over n subjects, and let Z denote an additional group membership variable; for example ethnicity, gender or clinical facility. We focus for simplicity on a scalar Z . We seek to estimate \tilde{X} , an $n \times p$ reconstructed version of the data matrix that is orthogonal to Z with minimal information loss. In our setting, the reconstructed version is used to produce a prediction rule $\hat{y}(\tilde{x})$ that returns a prediction of y for any input \tilde{x} . Our aim is to guarantee that $\hat{y}(\tilde{x})$ is uncorrelated with the group variable. In the sequel, we refer to this condition generically as “independent”.

We will focus on statistical models linear in the covariates, such as generalised linear models, support vector machines with linear kernels, and many others. It is easy to check that when $\hat{y}(\tilde{x})$ is a linear function of \tilde{x} , $\text{cov}(\hat{Y}, Z) = 0$ naturally follows from $\text{cov}(\tilde{X}, Z) = 0$. A natural procedure to transform the original data, then, consists in imposing orthogonality between \tilde{X} and Z , while attempting to preserve as much of the information in X as possible. The former requirement is geometrically analogous to requiring that the projection of z onto the range of the reconstructed covariates \tilde{X} is null.

In terms of the geometry of least squares estimation, the orthogonality condition guarantees that the columns of \tilde{X} provide no information about the variable Z (Hastie and Tibshirani, 2009). This assumption implies that it is not possible to predict the group membership using the transformed variables as covariates in a statistical model which is linear in the covariates. Potentially, non-linear dependencies could still be present in the transformed matrix \tilde{X} , and hence affect predictions of non-linear models. Our method can be motivated as a second-order adjustment, which attempts to accommodate for effects that are simple to measure and generally more relevant. As we will illustrate, in our experience higher order dependencies are often relatively modest in concrete applications, and our procedure also performs well when non-linear models are employed.

In high-dimensional settings, it is often assumed that large collections of variables have approximately a low-rank representation, meaning that observations lie close to a lower-dimensional subspace that captures the most salient properties of the data. We express the reduced rank approximation as $\tilde{X} = SU^T$, where U is a $p \times k$ matrix of k linear orthonormal basis vectors and S is the $n \times k$ matrix of associated scores.

The problem of preprocessing the data to ensure Orthogonality to Groups (henceforth OG) can be expressed as a minimization of the Frobenius distance between the original data and the approximated version, $\|X - \tilde{X}\|_F^2$, under the constraint $\langle \tilde{X}, Z \rangle = 0$. Given the particular structure assumed for \tilde{X} , this leads to the following optimization problem:

$$\arg \min_{S,U} \|X - SU^T\|_F^2, \quad \text{subject to } \langle SU^T, Z \rangle = 0, \quad U \in \mathcal{G}_{p,k} \quad (1)$$

where $\mathcal{G}_{p,k}$ is the Grassman manifold of orthonormal matrices.

Since the constraints are separable, it is possible to reformulate Equation (1) as p distinct constraints, one over each column of \tilde{X} . Moreover, since any column of \tilde{X} is a linear combination of the k columns of S , and U is orthonormal, the p constraints over \tilde{X} can be equivalently expressed as k constraints over the columns of the score matrix S . The matrix U is forced to lie on the Grassman manifold to prevent degenerate conditions, such as basis vectors being identically zero or solutions with double multiplicity.

The optimisation problem admits an equivalent formulation in terms of Lagrange multipliers,

$$\arg \min_{S,U} \left\{ \frac{1}{n} \sum_{i=1}^n \|x_i - \sum_{j=1}^k s_{ij} u_j^T\|^2 + \frac{2}{n} \sum_{j=1}^k \lambda_j \sum_{i=1}^n s_{ij} z_i \right\}, \quad (2)$$

with the introduction of the factor $2/n$ for ease of computation.

2.2 Theoretical support

The following Lemma characterizes the solution of the Orthogonal to Groups (OG) optimization problem, which can be interpreted as the residual of a multivariate regression among left singular values and a group variable. Let $V_k \Sigma_k U_k^T$ denote the rank- k singular values decomposition of X .

Lemma 2.1. *The problem stated in Equation (1) can be solved exactly, and admits an explicit solution in terms of singular values. The solution is equal to $\tilde{X} = (I_n - P_Z) V_k \Sigma_k U_k^T$, with $P_Z = Z(Z^T Z)^{-1} Z^T$.*

All proofs are given in Appendix A. The computational cost of the overall procedure is dominated by the cost of the partial singular value decomposition. This can be computed with modern methods in $O(nk^2)$ (Golub and Van Loan, 2012). The procedure outlined in Lemma 2.1 is simple and only involves matrix decomposition and least squares theory; hence we can fully characterise the solution and its properties. The following Lemma characterises the proposed solution within the class of constrained low-rank representations.

Lemma 2.2. *The solution \tilde{X} of the orthogonal to group algorithm is the best rank- k approximation, in Frobenius norm, of the data matrix X under the OG constraint.*

The singular value decomposition achieves the minimum error in Frobenius distance among all matrices of rank- k (e.g., Golub and Van Loan, 2012). Naturally, the introduction of additional constraints reduces the accuracy of the approximation, with respect to the optimal one. The following result allows us to bound the additional error analytically.

Lemma 2.3. *Let $\tilde{X}_k = V_k D_k U_k^T$ denote the best rank- k approximation of the matrix X obtained from the partial singular value decomposition of rank k . The reconstruction error of the OG algorithm is lower bounded by the optimal error rate of \tilde{X}_k , and the amount of additional error is equal to $\|P_Z V_k D_k\|_F^2$, where $P_Z = Z(Z^T Z)^{-1} Z^T$.*

The additional reconstruction error can be interpreted as a measure of the collinearity between the subspace spanned by Z and the left singular vectors of the data X . The more collinear the singular vectors are with the group variable, the greater is the amount of additional error with respect to the solution without the OG constraint. When these quantities are already orthogonal, then the solution is identical to the truncated singular value decomposition and the reconstruction achieves the minimum error.

2.3 Sparse OG procedure

In order to reduce the solution to a more interpretable structure, common methods in multivariate analysis impose constraints over the elements of a matrix decomposition, usually through an ℓ_1 -norm penalty to favour sparsity (e.g. Zou et al., 2006; Jolliffe et al., 2003; Witten et al., 2009). Besides improving the interpretability of the results, constraints improve the numerical estimation of the eigenvectors, which can be problematic in very high-dimensional applications (Johnstone, 2001).

To make the OG problem tractable and stable when the number of features is very large – potentially larger than the number of observations – we introduce additional constraints in the algorithm. We will build our method on a standard procedure to perform sparse matrix decomposition (e.g. [Hastie et al., 2015](#), Chapter 8), and adapt the computations to introduce the orthogonality constraint. We define the sparse orthogonal to group (SOG) optimization problem as follows.

$$\begin{aligned} & \arg \min_{S, U} \|X - SU^T\|_F^2 \\ \text{subject to } & \|u_j\|_2 \leq 1, \|u_j\|_1 \leq t, \|s_j\|_2 \leq 1, s_j^T s_l = 0, s_j^T Z = 0, \end{aligned} \quad (3)$$

for $j = 1, \dots, k$ and $l \neq j$. The problem in Equation (3) includes sparsity constraints over the vectors u_j and imposes orthogonality constraints among the score vectors s_j and the group variable, since the reconstructed version of $\tilde{X} = SU^T$ is a linear combination of the vectors s_j .

Focus now on the case of rank-1 approximation. As outlined in [Witten et al. \(2009\)](#), it is possible to show that the solutions in s and u for Equation (3) when $k = 1$ also solve

$$\arg \max_{s, u} s^T X u \quad \text{subject to } \|u\|_2 \leq 1, \|u\|_1 \leq t, \|s\|_2 \leq 1, s^T Z = 0. \quad (4)$$

Although the minimisation in Equation (4) is not jointly convex in s and u , it can be solved with an iterative algorithm. Since the additional constraints do not involve the vector u , when s is fixed the minimisation step is mathematically equivalent to a sparse matrix decomposition with constraints on the right singular vectors, and takes the following form.

$$\arg \max_u b u \quad \text{subject to } \|u\|_2 \leq 1, \|u\|_1 \leq t, \quad (5)$$

with $b = s^T X$ and solution equal to

$$u = g(b, \theta) = \frac{\mathcal{S}_\theta(b)}{\|\mathcal{S}_\theta(b)\|_2},$$

where \mathcal{S}_θ is the soft threshold operator, defined as $\mathcal{S}_\theta(x) = \text{sign}(x)(|x| - \theta)\mathbb{I}(|x| \geq \theta)$ and applied over every element separately. The value of θ is 0 if $\|b\|_1 \leq t$, and otherwise $\theta > 0$ is selected such that $\|g(b, \theta)\|_1 = t$ ([Hastie et al., 2015](#); [Witten et al., 2009](#)).

When u is fixed, the problem is similar to the solution described in Section 2.2, after arranging

Equation (4) as follows.

$$\arg \max_S s^T a \quad \text{subject to} \quad \|s\|_2 \leq 1, \quad s^T Z = 0, \quad (6)$$

with $a = Xu$. The solution to Equation (6) is directly related to the method outlined in Section 2.2, and is given by the following expression.

$$s = \frac{a - \beta Z}{\|a - \beta Z\|_2},$$

with $\beta = (Z^T Z)^{-1} Z^T a$.

Solutions with rank greater than 1 are obtained by consecutive univariate optimisation. For the j -th pair (u_j, s_j) , $j = 2, \dots, k$, the vector a of the partial problem outlined in Equation (4) is replaced with $P_{k-1}Xu_j^T$, where $P_{k-1} = I_{n \times n} - \sum_{l=1}^{k-1} s_l s_l^T$ projects Xu_j^T onto the complement of the orthogonal subspace $\text{span}(s_1, \dots, s_{k-1})$, thus guaranteeing orthogonality among the vectors s_j , $j = 1, \dots, k$. A detailed description of the algorithm outlined above is given in the Appendix A.

3 SIMULATION STUDY

We conduct a simulation study to evaluate the empirical performance of the proposed algorithms. The focus of the simulation is on assessing the fidelity in recovering a high-dimensional data matrix and success in removing the influence of the group variable from predictions for future subjects. We set $n = 5000$, $p = 200$, $k = 10$, and construct a loading matrix S , with size (n, k) , and a score matrix W with size (k, p) , with entries sampled from independent normal distributions. A group variable Z of length n is sampled from independent Bernoulli distributions with probability equal to 0.5. Each p -dimensional row of the $n \times p$ data matrix X is drawn from a p -variate standard normal distribution with mean vector $\mu_i = (s_i - 2z_i 1_k^T)W$, $i = 1, \dots, n$. Lastly, a synthetic continuous response y_i , $i = 1, \dots, n$ is sampled from independent Normal random variables with mean $(s_i - 2z_i 1_k^T)\beta$ and elements of β sampled uniformly in $(-5, 5)$. We evaluate two aspects of performance: accuracy of the approximation of X by \tilde{X} and success in achieving $\langle \hat{Y}, Z \rangle \approx 0$, where \hat{Y} is the prediction for Y estimated from \tilde{X} .

The left-panel (a) of Figure 1 illustrates the relative error between the reconstructed and original data, measured in terms of Frobenius distance for increasing values of the approximation rank k , and normalised with the Frobenius norm of X . As expected, for every value of k , the truncated SVD provides the reconstruction with minimum error. The approximation provided by the OG algorithm is competitive

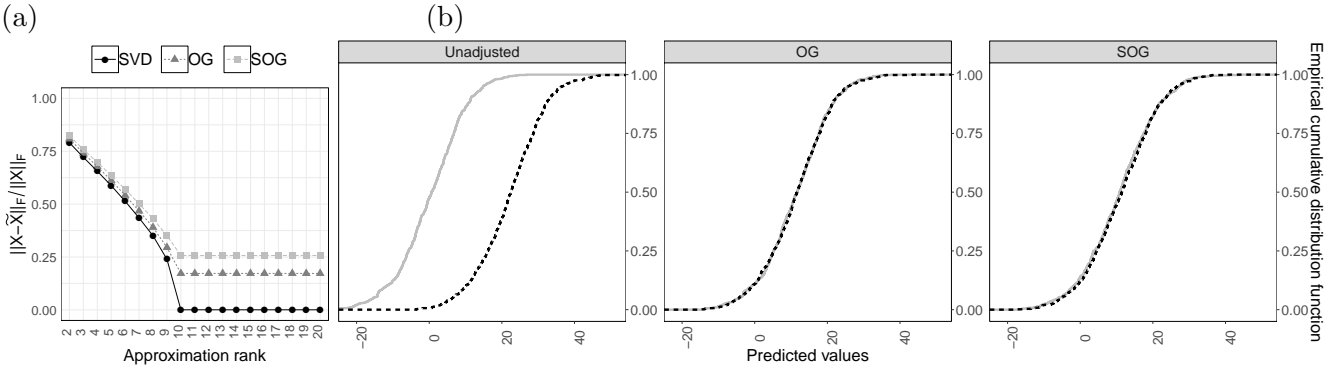


Figure 1: (a) Frobenius norm of the reconstruction error under three different matrix approximation. (b) Conditional cumulative distribution functions for \hat{Y} in the simulation study. Light solid gray refers to $Z = 1$, dotted black to $Z = 0$.

with the optimal reconstruction, and the relative improvement of the latter increases with the rank until the true value $k = 10$ is reached, and remains constant afterwards. This behaviour is not surprising, since the simulation setting for X suggests that the singular values σ_k for $k > 10$ are nearly 0, not affecting the quantity in Lemma 2.3. Moreover, although there are no theoretical guarantees on the error achieved with the SOG algorithm, in this simulation study its performance is numerically comparable to the performance of the OG algorithm.

Panel (b) in Figure 1, compares the empirical distribution of the out of sample predictions for $\hat{Y} \mid Z = 0$ and $\hat{Y} \mid Z = 1$, under different approaches. Data have been divided into a training and a test set, and a standard linear regression estimated on the training data is used to predict the outcome \hat{Y} on the remaining part. The dimensionality of the matrix X was reduced using the OG and SOG algorithms, using an approximation rank $k = 10$.

In the first panel, the predictive model was estimated over the ordinary SVD decomposition. Without adjustment, the distributions of the predicted values differ markedly as a function of Z , with the predictions for $Z = 1$ more concentrated at low values and predictions with $Z = 0$ at high values. The second and third panel illustrate the effect of removing the influence of the group Z with the SO algorithm and SOG algorithm, respectively. After removing the effect of the group variable Z from the transformed features \tilde{X} , predictions across different values of Z are similar in terms of their empirical distribution, with the conditional empirical cumulative distribution function matching almost perfectly.

4 APPLICATION

4.1 *Human connectome project*

Our motivating application is drawn from a study of the Human Connectome Project (HCP) on $n = 1056$ adult subjects (Glasser et al., 2016, 2013). The study provides, for each individual, information on the structural interconnections among the 68 brain regions characterizing the Desikan atlas (Desikan et al., 2006), measured through a combination of diffusion and structural magnetic resonance imaging (Zhang et al., 2018). Many different features are also available, covering a wide range of biographical, physiological and behavioural information at the individual level and technical information related to the specific session in which brain scans were collected. For an extended description of the Humane Connectome Project, the tools involved in the collection process and the aims of the study see Zhang et al. (2018); Glasser et al. (2016, 2013). For our purposes, it is enough to characterize the outcomes of interest as physiological and behavioural traits and the covariates as data on the presence and strength of connections between the 68 brain regions.

Recent developments in neuroscience and novel preprocessing pipelines have stimulated considerable interest in analysing the relation among brain structure/activity and subject-specific traits, with the main focus on detecting if variations in the brain structure are associated with variation in phenotypes (e.g. Genovese et al., 2002; Zhang et al., 2018; Durante and Dunson, 2018). Our specific focus is on investigating the relation between brain structural connectivity patterns and “hard” drug consumption, in order to establish whether the latter can be predicted on the basis of information recorded in the brain scans. There is evidence for the existence of brain differences across subjects with severe drug addictions, both in terms of functional connectivity (Wilcox et al., 2011; Kelly et al., 2011) and volumes (Beck et al., 2012; Goldstein et al., 2009). As discussed in Section 1, a fundamental problem with observational medical data is the presence of spurious or nuisance associations. In neuroscience, harmful factors that can negatively impact on predictive modelling include subject motion, eye movements, different protocols and hardware-specific features, among many others (Basser and Jones, 2002; Sandrini et al., 2011).

In the motivating application, a binary variable y_i indicates a positive result for subject i to a drug test for at least one among Cocaine, Opiates, Amphetamines, MethAmphetamine and Oxycontin. We regard the machine on which the data were gathered as the group variable whose influence we want to remove.

For every observation, a binary variable z_i indicates which scanner had recorded the i -th observation. In order to apply our proposed method, the brains scans were vectorised into a $n \times p$ matrix X , with $p = 2278$ corresponding to the vectorised numerical data on the strength of connection among all pairs of brain regions.

Predictive performance for the different approaches is evaluated over an independent test set, randomly sampled from the original data. In order to reduce the randomness from a single split, the results are averaged over 300 different splits into training and test. As a preliminary approach, analyses are conducted with two different naive approaches: using the original covariates, and including the scanner id variable z as a covariate. The first and second columns of Section 4.1 represent, respectively, results for a logistic regression using standard sparse SVD with 30 components (SVD) as covariates, and the same covariates including scanner as an additional covariate (SVD,Z). The third and fourth columns compare predictive performance for Lasso (Lasso(u)) and random forest (RF(u)), using all the unadjusted available covariates. Results suggest that predictions differ markedly across the two different scanners, and this issue equally affects both linear and non-linear models. This problem is exacerbated when the scanner id is used as a covariate. For example, classification error for observations in the second scanner is roughly two times greater than for the first one, suggesting that predictions are strongly related with the scanner used to collect data.

The right half of Section 4.1 shows results for the adjusted procedures. The fifth and sixth columns refer to predictions for a logistic regression estimated over 30 covariates extracted from the OG algorithm and its sparse version SOG, respectively. Predictions are now more similar across different scanners. For example, false negative rates are almost identical, and the global performance is comparable to the unadjusted setting. In addition, our methodology allows estimation of any baseline model on our pre-processed data. In the seventh column, a Lasso model has been estimated using data from the OG algorithm, although the results are worse than for the other baseline models. Although the proposed methods provide strong guarantees only for models which are linear in the covariates, the last column of Section 4.1 suggests that also a highly non-linear model (such as random forest) can obtain strong benefit from our methods. In this case, predictions across scanners are more similar, although less precise.

As a concluding check, we conducted separate Mann-Whitney tests to evaluate if the distribution of \hat{Y} is statistically different across different scanners. The null hypothesis of independence was not rejected

Table 1: Predictive performance on the HCP dataset for the approaches described in Section 4.1. S1 and S2 denote first and second scanner, respectively. Metrics: Classification Error, AUC, Accuracy, False negative rates, False positive rates.

			Unadjusted				Adjusted			
			SVD	SVD, Z	LASSO(u)	RF(u)	OG	SOG	LASSO	RF
CE	S1	0.302	0.266	0.161	0.454	0.293	0.312	0.403	0.451	
	S2	0.352	0.463	0.181	0.430	0.271	0.259	0.409	0.472	
AUC	S1	0.564	0.573	0.546	0.601	0.547	0.534	0.529	0.552	
	S2	0.647	0.631	0.644	0.714	0.547	0.552	0.552	0.621	
ACC	S1	0.608	0.644	0.749	0.456	0.617	0.598	0.507	0.459	
	S2	0.558	0.447	0.729	0.480	0.639	0.651	0.501	0.438	
FNR	S1	0.286	0.250	0.144	0.442	0.279	0.298	0.437	0.441	
	S2	0.313	0.430	0.154	0.392	0.241	0.222	0.427	0.441	
FPR	S1	0.015	0.016	0.017	0.012	0.014	0.014	0.010	0.010	
	S2	0.039	0.033	0.035	0.037	0.030	0.037	0.024	0.031	

for all the adjusted methods, and rejected for the unadjusted. We also conducted sensitivity analysis for different values of the approximation rank ranging in $\{10, 50, 100\}$, and results were consistent with the main empirical findings.

4.2 COMPAS recidivism data

As outlined in Section 1, another important area in which it is fundamental to remove unwanted association is criminal risk assessment. We will focus here on the COMPAS dataset, a standard dataset in the fairness literature which includes detailed information on criminal history for more than 6000 defendants over a time range of two years (Angwin et al., 2016). For each defendant, several features of criminal history are available, such as the number of past felonies, misdemeanors, and juvenile offenses. The defendants sex, age and race are also available. The focus of this example is on predicting two-year recidivism, with particular interest on providing predictions that are independent of race/ethnicity.

The design matrix X was constructed including the available features and all the interaction terms, for a total of 64 variables. Although the number of features is only moderately large, and considerably smaller than in the previous example, the use of approaches that requires manual intervention, such as Lum and Johndrow (2016), is burdensome. Moreover, the inclusion of every interaction term induces collinearity in the design matrix, thus motivating an approximation through a lower-dimensional structure.

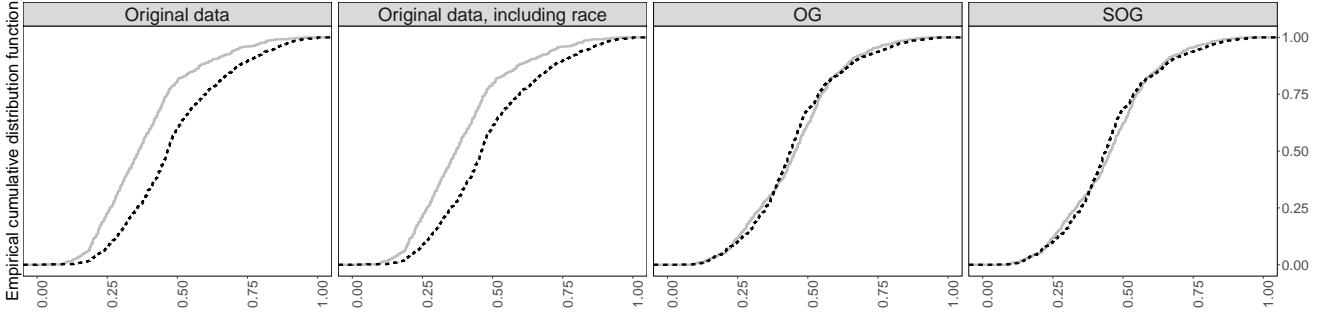


Figure 2: Empirical cumulative distribution functions for \hat{Y} under four approaches. Light solid gray refers to white ethnicity, dotted black to non-white.

Predictive performance for different competitors is evaluated over an independent test set, randomly sampled from the original data. Figure 2 compares the out-of-sample predictive distribution for four logistic regressions, trained on different data. The first two panels show unadjusted predictions, the first excluding racial information and the second using it as a covariate. Results show that Caucasian individuals (light continuous line) are systematically assigned lower probabilities of recidivism, at any level of the predicted risk. The third and fourth panels correspond, respectively, to predictions obtained from the OG and SOG algorithms, with $k = 10$. The gap between the two curves is notably reduced, both with the standard OG and the sparse implementation, leading to predictions which are more similar across different racial groups.

Table 2 reports results for the model previously described and other competitor approaches. The first and second columns of Table 2 represent, respectively, results for a logistic regression using all the available original covariates (OR) and all the variables and race (OR,Z). The third column (OR Z_0) corresponds to one approach discussed in [Pope and Sydnor \(2011\)](#), which consists in the estimation of a complete model with all the variables and race, and then setting to 0 the coefficient associated with group membership when predictions are performed. An alternative approach suggested in [Pope and Sydnor \(2011\)](#) consists in a full model estimation, and predictions obtained replacing z with its mean value \bar{z} in the test data. In this application, such approach leads to metrics identical to column (OR Z), and has not been reported.

The fourth and fifth columns compare predictive performance for Lasso (Lasso (u)) and random forest (RF(u)) respectively, using all the unadjusted available covariates. Numerical results suggest that predictions are strongly different across ethnic groups, and this issue affects both models linear and non-linear in the covariates. For example, the proportion of reoffenders correctly classified (TPR, true positive

rates) is roughly 1.5 times higher for white than for non-white subjects, and this issue holds for all the unadjusted approaches. Conversely, the True Negative Rate (TNR) is significantly lower for whites than for non-white individuals, suggesting that models estimated on the unadjusted features disproportionately assign low probabilities of recidivism to white subjects.

The second part of Table 2 illustrates results for the adjusted procedures. The sixth and seventh columns show results for a logistic regression estimated over 10 covariates extracted from the OG algorithm and its sparse version SOG, respectively, also reported in the third and fourth panel of Figure 2. The discrepancy in prediction metrics across racial group is less severe under these approaches. For example the True Positive Rate is increased and more similar across groups. Similarly to the brain scan application, results seems satisfactory also when a highly non-linear model is employed, such as a random forest in column (RF); predictive performance using the adjusted data is also on par with other articles that have analysed the same dataset (e.g. [Dieterich et al., 2016](#); [Lum and Johndrow, 2016](#)).

These empirical findings also highlight a compelling argument for using of the proposed method in risk assessment. Considering predictive performance of models with and without OG pre-processing, the values for Area Under the Roc curve and classification error before and after adjustment are very similar, in particular for the logistic regressions reported in Figure 2 and in the columns OR and OG, SOG in Table 2. This result suggests that, when interest is on predicting two-year recidivism, predictions from our methods achieve orthogonality from groups without large effects on the global accuracy.

DISCUSSION

In this article we proposed an efficient method to pre-process high-dimensional datasets to remove the influence of groups in predictive modelling. Our approach is simple, scalable, and has theoretical guarantees regarding approximation error and orthogonality from the group variables. Although the theoretical properties of the methods hold on models linear in the covariates, the empirical findings suggest that also when non-linear models are employed, the methods still work well, provide reasonable global predictive performance and predictions that are more similar across groups.

A promising future extension for the proposed method involves generalisation to more complex multi-dimensional data structures. For example, in the neuroscience application considered in Section 4.1, brain scans for multiple subjects can be represented as a 3-dimensional array, where every slice corresponds to

Table 2: Predictive performance on the COMPAS dataset for the approaches described in Section 4.2. W stands for White ethnicity, NW for the remaining ethnic groups. Metrics: Classification Error, AUC, Total positive Rate, Total Negative Rate, False negative rates, False positive rates.

		Unadjusted				Adjusted			
		OR	OR Z	OR Z_0	LASSO(u)	RF(u)	OG	SOG	LASSO
CE	W	0.281	0.285	0.281	0.303	0.285	0.329	0.329	0.344
	NW	0.318	0.316	0.316	0.321	0.325	0.333	0.333	0.332
AUC	W	0.734	0.734	0.734	0.715	0.725	0.722	0.722	0.717
	NW	0.729	0.729	0.729	0.720	0.733	0.731	0.731	0.732
TPR	W	0.569	0.562	0.569	0.534	0.577	0.453	0.453	0.434
	NW	0.401	0.408	0.419	0.389	0.428	0.434	0.434	0.447
TNR	W	0.150	0.153	0.150	0.163	0.138	0.218	0.218	0.221
	NW	0.282	0.276	0.266	0.290	0.247	0.233	0.233	0.221
FNR	W	0.045	0.052	0.045	0.080	0.037	0.161	0.161	0.180
	NW	0.123	0.116	0.105	0.135	0.096	0.089	0.089	0.077
FPR	W	0.236	0.233	0.236	0.223	0.248	0.168	0.168	0.165
	NW	0.194	0.200	0.211	0.186	0.229	0.244	0.244	0.255
									0.196

a brain network for a single subject (Zhang et al., 2018). The inclusion of constraints on orthogonality to groups can be accomplished adapting the contribution proposed in this article to some methods in tensor decompositions (e.g. Kolda and Bader, 2009).

A APPENDIX

Proof of Lemma 2.1. Focus on the case $k = 1$, where the approximation of the original set of data consists of finding the closest rank-1 matrix (vector). Equation (2) is reformulated as

$$\arg \min_{s_1, u_1} \left\{ \frac{1}{n} \sum_{i=1}^n \|x_i - s_{i1} u_1^T\|^2 + \frac{2}{n} \lambda_1 \sum_{i=1}^n s_{i1} z_i \right\}, \quad (7)$$

and some algebra and the orthonormal condition on u_1 allows us to express the loss function to be minimized as

$$\begin{aligned}
L(s_1, u_1) &= \frac{1}{n} \sum_{i=1}^n (x_i - s_{i1}u_1^T)^T (x_i - s_{i1}u_1^T) + \frac{2}{n} \lambda_1 \sum_{i=1}^n s_{i1} z_i \\
&= \frac{1}{n} \sum_{i=1}^n (x_i^T x_i - 2s_{i1} x_i u_1^T + s_{i1}^2) + \frac{2}{n} \lambda_1 \sum_{i=1}^n s_{i1} z_i.
\end{aligned}$$

The function is quadratic, and the partial derivative in s_{i1} leads to

$$\frac{\partial}{\partial s_{i1}} L(s_1, u_1) = \frac{1}{n} (-2x_i u_1^T + 2s_{i1}) + \frac{2}{n} \lambda_1 z_i,$$

with stationary point given by $s_{i1} = x_i u_1^T - \lambda_1 z_i$. The optimal score for the i -th subject is obtained by projecting the observed data onto the first basis, and then subtracting λ_1 -times z . The constraint does not involve the orthonormal basis u_1 , hence the solution of Equation (7) for u_1 is equivalent to the unconstrained scenario. A standard result of linear algebra states that the optimal u_1 for Equation (7) without constraints equivalent to the first right singular vector of X , or equivalently to the first eigenvector of the matrix $X^T X$ (e.g., [Hastie and Tibshirani, 2009](#)). Plugging in the solution for u_1 and setting the derivative with respect to λ_1 equal to 0 leads to

$$\sum_{i=1}^n (x_i u_1^T - \lambda_1 z_i)^T z_i = 0 \quad \lambda_1 = \frac{\sum_{i=1}^n x_i u_1^T z_i}{\sum_{i=1}^n z_i^2} = \frac{\langle X u_1^T, z \rangle}{\langle z, z \rangle}, \quad (8)$$

a least squares estimate of $X u_1^T$ over z .

Consider the complete problem formulated in Equation (2). The derivatives with respect to the generic element s_{ij} can be calculated easily due to the constraint $U \in G_{k,p}$, which simplifies the mixed products among the u_j s. The optimal solution for the generic score s_{ij} is given by

$$s_{ij} = x_i u_j^T - \lambda_j z_i, \quad (9)$$

since $u_i^T u_j = 0$ for all $i \neq j$ and $u_j^T u_j = 1$ for $j = 1, \dots, k$. The solution has an intuitive interpretation, since it implies that the optimal scores for the j -th dimension are obtained projecting the original data over the j -th basis, and then subtracting λ_j -times the observed value of z . Moreover, since the OG constraints do not involve any vector u_j , the optimization with respect to the basis can be derived from

known results in linear algebra. The optimal value for the vector u_j , with $j = 1, \dots, k$, is equal to the first k right singular values of X , sorted accordingly to the associated singular values (e.g., [Bishop, 2006](#); [Hastie et al., 2015](#)).

The global solution for $\lambda = (\lambda_1, \dots, \lambda_k)$ can be derived from least squares theory, since we can interpret Equation (9) as a multivariate linear regression where the k columns of the projected matrix XU^T are response variables and z a covariate. The general optimal value for λ_k is then equal to the multiple least squares solution

$$\lambda_k = \frac{\langle Xu_k^T, z \rangle}{\langle z, z \rangle}$$

□

Proof of Lemma 2.2. Since the optimization problem of Equation (1) is quadratic with a linear constraint, any local minima is also a global minima. The solution performed via the singular value decomposition and the least squares constitute a stationary point, that is also global minimum. □

Proof of Lemma 2.3. Let $V_k D_k U_k^T$ define the rank- k SVD decomposition of the matrix X , using the first k left and right singular vectors, and the first k singular values. Let \tilde{X}_{OG} define the approximated reconstruction obtained by the OG algorithm. The reconstruction error between the original data matrix X and its low-rank approximation \tilde{X}_{OG} can be decomposed as follow.

$$\begin{aligned} \|X - \tilde{X}_{OG}\|_F^2 &= \|X - (V_k D_k - Z\lambda)U_k^T\|_F^2 \\ &= \|X - V_k D_k U_k^T + Z\lambda U_k^T\|_F^2 \\ &= \|X - V_k D_k U_k^T\|_F^2 + \|Z\lambda U_k^T\|_F^2 + 2\langle X - V_k D_k U_k^T, Z\lambda U_k^T \rangle_F. \end{aligned}$$

The Frobenius-inner product term vanishes due to the orthogonality of the singular vectors, and rearranging terms the following expression is obtained.

$$\|X - \tilde{X}_{OR}\|_F^2 - \|X - V_k D_k U_k^T\|_F^2 = \|Z\lambda U_k^T\|_F^2 = \|Z\lambda\|_F^2,$$

Since the optimal value for λ is equal to the least squares solution of Z over $V_k D_k$, it follows that

$\|Z\lambda\|_F^2 = \|Z(Z^T Z)^{-1} Z^T V_k D_k\|_F^2$, and the proof is complete. \square

Algorithm 1: Sparse Orthogonal to Subgroup (SOG) algorithm

Input: Data matrix X

for $j = 1, \dots, k$ **do**

while *Changes in u_j and s_j are not sufficiently small* **do**

 Compute β_j via least squares as

$$\beta_j = (Z^T Z)^{-1} Z^T P_{j-1} X u_j,$$

 with $P_{j-1} = I_{n \times n} - \sum_{l=1}^{j-1} s_l s_l^T$

 Update $s_j \in \mathbb{R}^n$ as

$$s_j = \frac{P_{j-1} X u_j - \beta_j Z}{\|P_{j-1} X u_j - \beta_j Z\|_2}$$

 Update $u_j \in \mathbb{R}^p$ as

$$u_j = \frac{\mathcal{S}_\theta(X^T s_j)}{\|\mathcal{S}_\theta(X^T s_j)\|_2},$$

 where $\mathcal{S}_\theta(x) = \text{sign}(x)(|x| - \theta)\mathbb{I}(|x| \geq \theta)$ and

if $\|X^T s_j\|_1 \leq t$ **then**

 | Set $\theta = 0$

else

 | Set $\theta > 0$ such that $\|u_j\|_1 = t$

end

end

end

Output: Set $d_j = s_j^T X u_j$. Let S denote the $n \times k$ matrix with columns $d_j s_j$. Let U denote the $p \times k$ sparse matrix with rows u_j , $j = 1, \dots, k$. Return $\tilde{X} = S U^T$

REFERENCES

Angwin, J., Larson, J., Mattu, S., and Kirchner, L. (2016). Machine bias: There's software used across the country to predict future criminals. and it's biased against blacks. *ProPublica*.

Basser, P. J. and Jones, D. K. (2002). Diffusion-tensor mri: theory, experimental design and data analysis—

a technical review. *NMR in Biomedicine: An International Journal Devoted to the Development and Application of Magnetic Resonance In Vivo*, 15(7-8):456–467.

Beck, A., Wüstenberg, T., Genauck, A., Wräse, J., Schlagenhauf, F., Smolka, M. N., Mann, K., and Heinz, A. (2012). Effect of brain structure, brain function, and brain connectivity on relapse in alcohol-dependent patients. *Archives of general psychiatry*, 69(8):842–852.

Bishop, C. M. (2006). *Pattern recognition and machine learning*. Springer, New York.

Bridges, G. S. and Crutchfield, R. D. (1988). Law, social standing and racial disparities in imprisonment. *Social Forces*, 66(3):699–724.

Desikan, R., Ségonne, F., Fischl, B., Quinn, B., Dickerson, B., Blacker, D., Buckner, R., Dale, A., Maguire, R., and Hyman, B. (2006). An automated labeling system for subdividing the human cerebral cortex on mri scans into gyral based regions of interest. *Neuroimage*, 31:968–980.

Dieterich, W., Mendoza, C., and Brennan, T. (2016). Compas risk scales: Demonstrating accuracy equity and predictive parity. Technical report, Northpointe.

Dunson, D. B. (2018). Statistics in the big data era: Failures of the machine. *Statistics & Probability Letters*, 136:4–9.

Durante, D. and Dunson, D. B. (2018). Bayesian inference and testing of group differences in brain networks. *Bayesian Analysis*, 13(1):29–58.

Feldman, M., Friedler, S. A., Moeller, J., Scheidegger, C., and Venkatasubramanian, S. (2015). Certifying and removing disparate impact. *Proceedings of the 21th ACM SIGKDD International Conference on Knowledge Discovery and Data Mining*, pages 259–268.

Genovese, C. R., Lazar, N. A., and Nichols, T. (2002). Thresholding of statistical maps in functional neuroimaging using the false discovery rate. *Neuroimage*, 15(4):870–878.

Glasser, M. F., Smith, S. M., Marcus, D. S., Andersson, J. L., Auerbach, E. J., Behrens, T. E., Coalson, T. S., Harms, M. P., Jenkinson, M., Moeller, S., et al. (2016). The human connectome project’s neuroimaging approach. *Nature Neuroscience*, 19(9):1175–1187.

- Glasser, M. F., Sotiroopoulos, S. N., Wilson, J. A., Coalson, T. S., Fischl, B., Andersson, J. L., Xu, J., Jbabdi, S., Webster, M., Polimeni, J. R., et al. (2013). The minimal preprocessing pipelines for the human connectome project. *Neuroimage*, 80:105–124.
- Goldstein, R. Z., Bechara, A., Garavan, H., Childress, A. R., Paulus, M. P., Volkow, N. D., et al. (2009). The neurocircuitry of impaired insight in drug addiction. *Trends in cognitive sciences*, 13(9):372–380.
- Golub, G. H. and Van Loan, C. F. (2012). *Matrix computations*, volume 3. JHU Press.
- Hastie, T. and Tibshirani, R. (2009). The elements of statistical learning; data mining, inference and prediction.
- Hastie, T., Tibshirani, R., and Wainwright, M. (2015). *Statistical learning with sparsity: the lasso and generalizations*. CRC press.
- Johnstone, I. M. (2001). On the distribution of the largest eigenvalue in principal components analysis. *Annals of statistics*, pages 295–327.
- Jolliffe, I. T., Trendafilov, N. T., and Uddin, M. (2003). A modified principal component technique based on the lasso. *Journal of computational and Graphical Statistics*, 12(3):531–547.
- Kamiran, F. and Calders, T. (2012). Data preprocessing techniques for classification without discrimination. *Knowledge and Information Systems*, 33(1):1–33.
- Kelly, C., Zuo, X.-N., Gotimer, K., Cox, C. L., Lynch, L., Brock, D., Imperati, D., Garavan, H., Rotrosen, J., Castellanos, F. X., et al. (2011). Reduced interhemispheric resting state functional connectivity in cocaine addiction. *Biological psychiatry*, 69(7):684–692.
- Kolda, T. G. and Bader, B. W. (2009). Tensor decompositions and applications. *SIAM review*, 51(3):455–500.
- Lum, K. (2017). Limitations of mitigating judicial bias with machine learning. *Nature Human Behaviour*, 1(7):s41562–017.
- Lum, K. and Isaac, W. (2016). To predict and serve? *Significance*, 13(5):14–19.

- Lum, K. and Johndrow, J. (2016). A statistical framework for fair predictive algorithms. *arXiv preprint arXiv:1610.08077*.
- Obermeyer, Z. and Emanuel, E. J. (2016). Predicting the future - big data, machine learning, and clinical medicine. *The New England journal of medicine*, 375(13):1216.
- Pope, D. G. and Sydnor, J. R. (2011). Implementing anti-discrimination policies in statistical profiling models. *American Economic Journal: Economic Policy*, 3(3):206–31.
- Raghunathan, T. E., Reiter, J. P., and Rubin, D. B. (2003). Multiple imputation for statistical disclosure limitation. *Journal of official statistics*, 19(1):1.
- Reiter, J. P. (2005). Releasing multiply imputed, synthetic public use microdata: An illustration and empirical study. *Journal of the Royal Statistical Society: Series A (Statistics in Society)*, 168(1):185–205.
- Rudovsky, D. (2001). Law enforcement by stereotypes and serendipity: Racial profiling and stops and searches without cause. *U. Pa. J. Const. L.*, 3:296.
- Sandrini, M., Umiltà, C., and Rusconi, E. (2011). The use of transcranial magnetic stimulation in cognitive neuroscience: a new synthesis of methodological issues. *Neuroscience & Biobehavioral Reviews*, 35(3):516–536.
- Simoiu, C., Corbett-Davies, S., and Goel, S. (2017). The problem of infra-marginality in outcome tests for discrimination. *The Annals of Applied Statistics*, 11(3):1193–1216.
- Wang, S. and Summers, R. M. (2012). Machine learning and radiology. *Medical image analysis*, 16(5):933–951.
- Wilcox, C. E., Teshiba, T. M., Merideth, F., Ling, J., and Mayer, A. R. (2011). Enhanced cue reactivity and fronto-striatal functional connectivity in cocaine use disorders. *Drug and alcohol dependence*, 115(1-2):137–144.
- Witten, D. M., Tibshirani, R., and Hastie, T. (2009). A penalized matrix decomposition, with applications to sparse principal components and canonical correlation analysis. *Biostatistics*, 10(3):515–534.

Zech, J. R., Badgeley, M. A., Liu, M., Costa, A. B., Titano, J. J., and Oermann, E. K. (2018). Confounding variables can degrade generalization performance of radiological deep learning models. *arXiv preprint arXiv:1807.00431*.

Zhang, Z., Allen, G., Zhu, H., and Dunson, D. B. (2018). Relationships between human brain structural connectomes and traits. *bioRxiv*, page 256933.

Zou, H., Hastie, T., and Tibshirani, R. (2006). Sparse principal component analysis. *Journal of computational and graphical statistics*, 15(2):265–286.